

Evolution of the order parameter after bubble collisions

Edward W. Kolb*

*NASA/Fermilab Astrophysics Center, Fermi National Accelerator Laboratory, Batavia, Illinois 60510
and Department of Astronomy and Astrophysics, Enrico Fermi Institute, The University of Chicago, Chicago, Illinois 60637*

Antonio Riotto†

NASA/Fermilab Astrophysics Center, Fermi National Accelerator Laboratory, Batavia, Illinois 60510

Igor I. Tkachev‡

*Department of Physics, The Ohio State University, Columbus, Ohio 43210
and Institute for Nuclear Research of the Academy of Sciences of Russia, Moscow 117312, Russia*

(Received 19 March 1997)

If a first-order phase transition is terminated by percolation and collisions of new-phase bubbles, there will exist a period of nonequilibrium between the time bubbles collide and the time thermal equilibrium is established. We study the behavior of the order parameter during this phase. We find that large nonthermal fluctuations at this stage reduce the order parameter below its eventual thermal equilibrium value. We comment on possible consequences for electroweak baryogenesis. [S0556-2821(97)04422-6]

PACS number(s): 98.80.Cq, 11.27.+d

It has long been known that symmetry may be restored at high temperature in local thermodynamic equilibrium (LTE) [1]. Recently it was realized that certain nonequilibrium (NEQ) conditions can be even more efficient for symmetry restoration [2]. An example of such a nonequilibrium state can arise naturally after inflation in the so-called preheating era [3,4]. In fact, symmetry may be restored in the NEQ state even if it is not restored in the LTE state formed by thermalization of the NEQ state. Detailed numerical studies [5] confirm that fluctuations of inflaton decay products are large enough for symmetry restoration, as well as for several other important effects, including baryogenesis [6], supersymmetry breaking [7], and generation of a background of relic gravitational waves [8].

States with properties similar to those in preheating, namely, anomalously large fluctuations and highly NEQ conditions, can arise in other situations as well. It was suggested in Ref. [9] that if bubble collisions produce large numbers of soft scalar particles carrying quantum numbers associated with a spontaneously broken symmetry, the phenomenon of (or tendency toward) symmetry restoration may occur locally in regions of high density of the soft quanta. The basic point is that bubble collisions create NEQ conditions with a large number of “soft” quanta of average energy smaller than the equivalent LTE temperature corresponding to instantaneous conversion of the bubble energy density into radiation. Since it may require several scattering times for the low-energy quanta to form a thermal distribution, it is rather reasonable to consider the NEQ period as a separate epoch. This may be referred to as a “preheating” epoch in a manner similar to the preheating phase of slow-roll inflation.

The effect of NEQ conditions after bubble collisions may be readily understood by the following (somewhat oversimplified) reasoning. Let us imagine that particles χ are produced in the bubble wall collisions and are charged under some symmetry group, so that their mass m_χ depends upon some scalar field ϕ (the order parameter of the symmetry) as $m_\chi^2(\phi) = m_0^2 + g\phi^2$.¹ Here, g represents a combination of numerical factors and a coupling constant. As a simple example we might assume that the ϕ -dependent mass originates from a potential term of the form $V_{\chi\phi} = (1/2)g\phi^2\chi^2$. As opposed to the large-angle scattering processes required for thermalization, forward-scattering processes do not alter the distribution function of the particles, but simply modify the dispersion relation. This is true in NEQ conditions, as well as the familiar LTE conditions. Forward scattering is manifest, for example, as ensemble and scalar background corrections to the particle masses. Since the forward-scattering rate is usually larger than the large-angle scattering rate responsible for establishing a thermal distribution, the nonequilibrium ensemble and scalar background corrections are present before the initial distribution function relaxes to its thermal value. These considerations allow us to impose the dispersion relation $\omega^2 = \mathbf{p}^2 + m_\chi^2(\phi)$ for NEQ conditions.

The leading contribution of the particles created by bubble collisions to the one-loop effective potential of the scalar field ϕ can be shown to be $\Delta V(\phi) \approx (n/E)m_\chi^2(\phi)$ [2,10], where n and E are the number density and the energy of the χ quanta, respectively. We may write the potential for the NEQ configuration as $\Delta V(\phi) = B_{\text{NEQ}}\phi^2$, where $B_{\text{NEQ}} = gn/E$. In NEQ conditions, the coefficient B_{NEQ} may

*Electronic address: rocky@rigoletto.fnal.gov

†Electronic address: riotto@fnas01.fnal.gov

‡Electronic address: tkachev@wollaston.mps.ohio-state.edu

¹Of course χ particles may coincide with the ϕ particles themselves, but in this example the colliding bubbles are *not* made from the field ϕ . Otherwise, there can be some effect, but the original symmetry will not be restored.

be quite large, indeed larger than the corresponding equilibrium coefficient which scales like T_{LTE}^2 , T_{LTE} defined as the temperature of the universe when the thermal spectrum of radiation is first obtained. Therefore, the tendency of symmetry restoration may turn out to be rather independent of T_{LTE} . We also notice that since the energy E scales like the inverse of the bubble wall width Δ , $E \sim \Delta^{-1}$, one can suggest that the effect of soft particles on symmetry restoration is stronger for thick bubble walls.

The aim of the present paper is to investigate numerically the effect of NEQ conditions following bubble wall collisions. We will show explicitly that at the final stage of first-order phase transitions when percolation and bubble collisions occur nonthermal quanta are produced and that they tend to shift the order parameter ϕ from its equilibrium value toward smaller values. We will also confirm the conjecture about the dependence of the strength of symmetry restoration upon the bubble wall width. Finally, we will comment on the possible implications that our result may have for electroweak baryogenesis.

Let us concentrate on a theory with a single scalar field ϕ (the χ particles of the above discussions must be identified with the ϕ) with Lagrangian density

$$\mathcal{L} = \frac{1}{2} \partial \phi_\mu \partial \phi^\mu - \frac{1}{2} m^2 \phi^2 + \frac{1}{3} c \phi^3 - \frac{1}{4} \lambda \phi^4 - V_0, \quad (1)$$

where V_0 is a constant. We introduce the dimensionless variables $\varphi \equiv \phi/\phi_0$, $\tau \equiv \sqrt{\lambda} \phi_0 t$, and $\xi \equiv \sqrt{\lambda} \phi_0 x$, where ϕ_0 will be fixed later. In the new variables the factor $\lambda \phi_0^4$ is an overall multiplication factor for the Lagrangian ($\tilde{m} = m/\sqrt{\lambda} \phi_0$, $\tilde{c} = c/\lambda \phi_0$, $\tilde{V}_0 = V_0/\lambda \phi_0^4$)

$$\begin{aligned} \mathcal{L} &= \lambda \phi_0^4 \left[\frac{1}{2} \partial \varphi_\mu \partial \varphi^\mu - \frac{1}{2} \tilde{m}^2 \varphi^2 + \frac{1}{3} \tilde{c} \varphi^3 - \frac{1}{4} \varphi^4 - \tilde{V}_0 \right] \\ &\equiv \lambda \phi_0^4 \left[\frac{1}{2} \partial \varphi_\mu \partial \varphi^\mu - V(\varphi) \right]. \end{aligned} \quad (2)$$

The overall factor will not enter the equation of motion. The final step is a choice of a potential, which we choose such that $dV/d\varphi = \varphi(\varphi-1)(\varphi-\varphi_m)$. The equation of motion is then

$$\square \varphi + \varphi(\varphi-1)(\varphi-\varphi_m) = 0. \quad (3)$$

With this choice of $dV/d\varphi$ the extrema of the potential are transparent: It has minima at $\varphi=0$ and $\varphi=1$ and a local maximum at $\varphi=\varphi_m$ (we thus fix the parameter φ_m to be in the range $0 < \varphi_m < 1$). We shall assume $\varphi=1$ corresponds to the true vacuum, i.e., $V(0) > V(1)$. Making the connection with Eq. (1), we conclude that $\phi = \phi_0$ is the field strength in the true vacuum, and the constants entering Eq. (1) are $m^2 = \varphi_m \lambda \phi_0^2$ and $c = (1 + \varphi_m) \lambda \phi_0$. We shall require the absence of a cosmological constant in the true vacuum, $V(1) = 0$; this gives $V_0 = (1 - 2\varphi_m) \lambda \phi_0^4 / 12$. Since we consider the true vacuum to be at $\varphi=1$ and the false vacuum at $\varphi=0$, we can further restrict the parameter φ_m to be in the range $0 < \varphi_m < 0.5$. We choose $\varphi_m = 0.1$ for the only param-

eter in the equation of motion, which implies that the physical mass of the scalar field in the true vacuum will be $m_\phi^2 = (1 - \varphi_m) \lambda \phi_0^2 = 0.9 \lambda \phi_0^2$.

The fact that only one parameter φ_m enters the equation of motion in the rescaled variables is a key point. The evolution of any initial field configuration $\varphi(\tau=0, \xi)$ for fixed φ_m will be the same in the rescaled variables, regardless of the coupling constant λ .

The initial field configuration for the problem at hand corresponds to a set of new-phase critical bubbles expanding in the false vacuum. Note that the evolution of a critical bubble is also defined by Eq. (3), and consequently it is fixed when φ_m is fixed. However, the bubble nucleation probability is a more complicated function of the other variables (note that nucleation became unsuppressed when $\varphi_m \rightarrow 0$, i.e., when the potential barrier disappears). The nucleation probability will determine the initial separation of critical bubbles (in space, as well as in time). In our numerical integration we will consider the mean separation of bubble nucleation sites as another free parameter of the model. Fixing it gives one extra constraint on the set of parameters λ , ϕ_0 , and φ_m .

After nucleation, new-phase bubbles expand, percolate, and collide. After collisions the spatial distribution of the magnitude of φ resembles a random superposition of many wavelength modes—a configuration with large field fluctuations. It is important that the system is classical and can be described by Eq. (3) from the time of bubble nucleation, through the time of bubble collisions and the condition of large field fluctuations.

The random-wave configuration is quickly established after bubble collisions; essentially it is established on the time scale of bubble collisions since there is no small parameters in Eq. (3). Eventually the waves interact and LTE is established. Since transforming the NEQ distribution function into an LTE distribution function involves producing states with small occupation number, the coupling constant λ will enter the time scale for the establishment of LTE. This time scale can be very long if λ is small, and so the NEQ configuration can exist for a long time. This phase has specific properties which are the subject of our study here.

First, let us recall what is expected in the final LTE state. The LTE temperature can be found using energy conservation

$$g_* \frac{\pi^2}{30} T_{\text{LTE}}^4 = V_0 = \lambda \phi_0^4 \frac{(1 - 2\varphi_m)}{12}, \quad (4)$$

which gives

$$T_{\text{LTE}} = \left(\frac{\lambda}{g_*} \right)^{1/4} \phi_0 \left[\frac{5(1 - 2\varphi_m)}{\pi^2} \right]^{1/4} \equiv \lambda^{1/4} \phi_0 b, \quad (5)$$

where b is a constant of order unity and $g_*(T)$ is the number of relativistic degrees of freedom at temperature T . Note that T_{LTE} approaches zero as λ approaches 0. Because of interactions with the medium, LTE values of the model parameters, e.g., the effective mass, are different than vacuum values. The value of the parameters can be calculated as loop corrections to the action. Most important is the change of the effective mass, $m_{\text{eff}}^2(T) = m^2 + \lambda T^2/4$. At very high temperatures $m_{\text{eff}}^2(T)$ becomes positive, even if the zero-temperature

value of m^2 was negative. This is a signal that broken symmetries are restored at high temperatures [1].

In the model of Eq. (1) which we consider here, the symmetry cannot be restored again after bubble collisions, but the temperature-dependent contribution to the effective mass will be nonzero. Using Eq. (5) we find that it scales with coupling constant as $\lambda^{3/2}$, and tends to zero as λ tends to 0. Note for what follows that the temperature-dependent correction to the mass can be written in more general form, as $m_{\text{eff}}^2 = m^2 + 3\lambda\langle\phi^2 - \langle\phi\rangle^2\rangle$.

Let us now find the mean value of the field ϕ in thermal equilibrium with temperature given by Eq. (5). To leading order in the coupling constants, the equation $dV_{\text{eff}}/d\phi = 0$ becomes

$$(\varphi_m + 3\sqrt{\lambda}b^2)\varphi - (1 + \varphi_m)\varphi^2 + \varphi^3 - (1 + \varphi_m)\sqrt{\lambda}b^2/12 = 0, \quad (6)$$

where terms proportional to $\sqrt{\lambda}$ are reminiscent of temperature-dependent corrections to the effective potential rewritten in terms of our dimensionless variables. We see that the solution of this equation tends to $\varphi = 1$ when $\lambda \rightarrow 0$. In other words, the mean value of the field ϕ in thermal equilibrium (established after the phase transition is completed) differs very little from the vacuum expectation value if the coupling constant is small.

We can study the process of bubble collisions and subsequent chaotization by numerically integrating Eq. (3). We are not interested in the collision of two isolated bubbles, but in the nearly simultaneous collisions of many bubbles, as might be expected at the end of a cosmological first-order phase transition. Rather than track the evolution of many bubbles, by use of periodic boundary conditions we can simulate the desired situation starting with a single bubble.

We define a three-dimensional box of size l on a grid of size 128^3 employing periodic boundary conditions. With periodic boundary conditions every bubble in the box is mirrored by its (infinitely repeating) reflections. As the bubble expands to fill the box, it will collide with its reflections, and so there is no need to put more than one bubble inside the box to study bubble collisions. Therefore we can study an initial configuration corresponding to just one critical bubble of the true phase in the box.

The size of the box, l , corresponds to the mean initial separation of bubbles in units of $(\lambda^{1/2}\phi_0)^{-1} \simeq m_\phi^{-1}$. We integrated the equation of motion for $l/2\pi = 4, 8, 10$, and 12 , corresponding to progressively larger bubbles at collision time. There is a practical limit on the size of the box set by the requirement that the bubble wall be able to be resolved. If the box is too large, then the bubble will grow large before colliding, and the wall will become too thin to resolve.

We show the evolution of a two-dimensional slice through the three-dimensional space of the simulation in Fig. 1 for the case $l/2\pi = 8$ as a function of time. [Time is expressed in units of $(\lambda^{1/2}\phi_0)^{-1} \simeq m_\phi^{-1}$.] The slice is centered on the bubble. The bubble was placed off center in the box to avoid numerical artifacts. The height above the plane corresponds to the value of the scalar field normalized to its vacuum value as discussed above (i.e., one corresponds to true vacuum and zero corresponds to false vacuum). The units in the plane indicate the spatial position, with each unit

from zero to $l = 16\pi \simeq 50$, corresponding roughly to an inverse mass of the scalar particle in the true vacuum.

At time equal to zero, a bubble is nucleated. The bubble shown is a solution to the equations of motion. When first nucleated, the scalar field at the center of the bubble is not in the true vacuum because it is a rather thick-wall bubble.

The slice corresponding to time $t = 15m_\phi^{-1}$ shows the growing bubble of true vacuum. Note that the bubble has gone out of the back and left-hand sides of the box and is now propagating inward from the front and right sides of the box toward the expanding bubble.

In the slice at $t = 30m_\phi^{-1}$, the bubble walls have just collided. The shallow and wide pockets at coordinates near the points (10,40) and (40,10) are regions that have been passed by true vacuum bubble walls—they are the debris of the collision. The deep pocket near coordinate (40,40) extends to the false vacuum—it is a region that has yet to experience the passing of a domain wall.

By $t = 45m_\phi^{-1}$ the entire box has been swept by a true-vacuum bubble wall. Eventually the system will evolve to the situation where the field is everywhere in the true vacuum ($\varphi = 1$) and the false-vacuum energy has been converted to a thermal bath of ϕ particles. But the situation at $t = 45m_\phi^{-1}$ and for the remainder of the simulation does not resemble that state. Before the ultimate thermal state is reached, there are large, long-wavelength field oscillations. The system is truly chaotic. Although at $t = 60m_\phi^{-1}$ the system appears to be approaching a quiescent state, at $t = 75m_\phi^{-1}$ and $t = 105m_\phi^{-1}$ there are large-amplitude, long-wavelength oscillations.

These large-amplitude, long-wavelength oscillations do not resemble a thermal background: The background is a true NEQ distribution, and the effect upon the zero-mode of the field, $\varphi_0 = \langle\varphi\rangle$, will be different than the effect of the background after thermalization. The nonthermal nature of the fluctuations can be quantified in terms of the power spectrum of the fluctuations of the scalar field φ . At any time the fluctuations can be expanded in terms of a Fourier series. We normalize the power spectrum of the fluctuations, $P_\varphi(k)$, in such a way that Parseval's theorem reads $\int d^3k P_\varphi(k) = L^{-3} \int d^3x [\varphi(x) - \varphi_0]^2 = \text{Var}(\varphi)$.

Using a fast Fourier transform, we monitored the power spectrum of fluctuations during the evolution of the system. The evolution of the power spectrum is illustrated in Fig. 2. The rescaled momentum k in this figure is related to the physical momentum, k_{phys} by $k_{\text{phys}} = \sqrt{\lambda}\phi_0 k \simeq m_\phi k$. For comparison we also plot on this figure the power spectrum of the field in LTE.

In LTE at temperature T , thermal fluctuations in the field are found by examining the finite-temperature, two-point correlation function. The two-point correlation function is given by the Green's function

$$\langle\phi(x)\phi(0)\rangle = \int \frac{d^4k}{(2\pi)^4} e^{-ikx} D_T(k), \quad (7)$$

where $D_T(k)$ is the ϕ propagator at finite temperature, given by

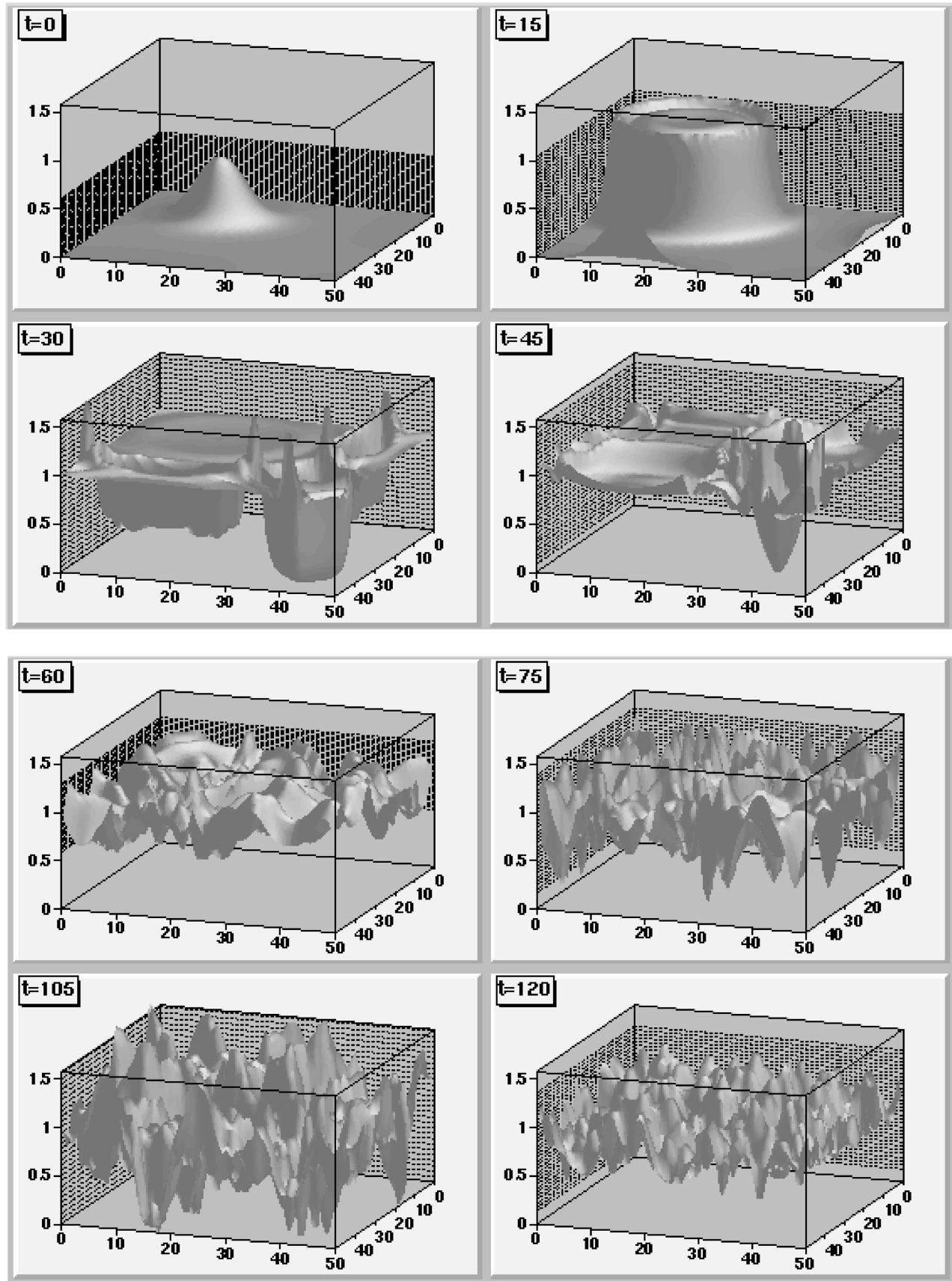


FIG. 1. A series of illustrations of the spatial dependence of the scalar field for a two-dimensional slice through the center of the bubble for the case $l/2\pi=8$. The height indicates the value of the scalar field normalized to the true vacuum value. Time and space are in units of $(\lambda^{1/2}\phi_0)^{-1}\simeq m_\phi^{-1}$. The details are discussed in the text.

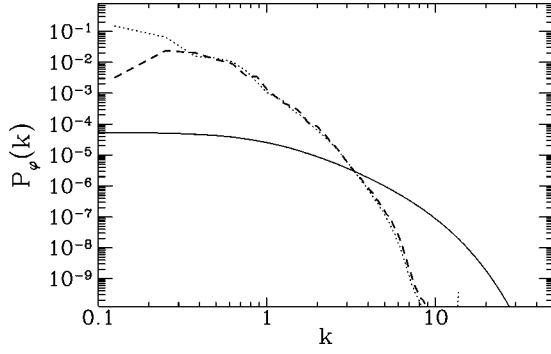


FIG. 2. The evolution of the power spectrum $P_\phi(k)$ of fluctuations in the ϕ field for $l/2\pi=8$. The dotted line is the spectrum when the bubbles have first completely collided ($t=45m_\phi^{-1}$), the dashed line is the spectrum well after bubble collision ($t=120m_\phi^{-1}$), and the solid line is a representative of the eventual thermal spectrum (here given for $\lambda=10^{-2}$).

$$D_T(k) = \frac{i}{k^2 - m_\phi^2 + i\epsilon} + 2\pi\delta(k^2 - m_\phi^2) \frac{1}{\exp(-E/T) - 1} \quad (8)$$

in the real-time formalism. The temperature-independent contribution is absorbed into the renormalization of the ϕ propagator, and the temperature-dependent part results in

$$\begin{aligned} \langle \phi(0)\phi(0) \rangle &= \int \frac{d^4k}{(2\pi)^4} \frac{2\pi\delta(k^2 - m_\phi^2)}{\exp(-E/T) - 1} \\ &= \int \frac{d^3k}{(2\pi)^3} \frac{1}{2E} \frac{1}{\exp(-E/T) - 1}. \end{aligned} \quad (9)$$

Choosing the same normalization of the power spectra for both the data and LTE, $P_\phi(k) = (2\pi)^{-3}(2E)^{-1}[\exp(E/T) - 1]^{-1}$, where $E^2 = m_\phi^2 + k_{\text{phys}}^2$. The LTE thermal fluctuations depend upon m_ϕ and the temperature. In turn, both depend upon λ . In Fig. 2 we give the power spectrum for thermal fluctuations at T_{LTE} , given by Eq. (5), for $\lambda=10^{-2}$.

We see from Fig. 2 that the power spectra of the random field after bubble collisions is much steeper than the LTE spectrum, with much more power on large-distance scales (small k). This again reflects our statement that $\text{Var}(\phi)$ right after the bubble collisions is much larger and much softer compared to LTE fluctuations. Note that the nonequilibrium state which we are discussing is long lived: The power spectra did not change appreciably during the time interval $60 < tm_\phi < 120$, and since the time needed to reach LTE is proportional to λ^{-2} , the NTE epoch is distinct, with peculiar properties which were neglected in previous discussions of phase transitions.

The results for the time dependence of zero mode of the field, $\varphi_0 = \langle \phi \rangle$, are presented in Fig. 3, where $\langle \dots \rangle$ means the spatial average (over grid points). We see that after bubbles have collided ($\tau > 16$ for $l/2\pi=4$ and $\tau > 40$ for $l/2\pi=8$), the zero mode does not relax to its vacuum value, $\varphi_0=1$, but oscillates near some smaller value. We define $\varphi_0 \equiv \langle \phi \rangle$, where the overbar denotes the time average over several oscillations. We find $\varphi_0 \approx 0.93$ in the case $l/2\pi=8$ and $\varphi_0 \approx 0.87$ with $l/2\pi=4$ at $\tau \sim 80$. Note that φ_0 rises

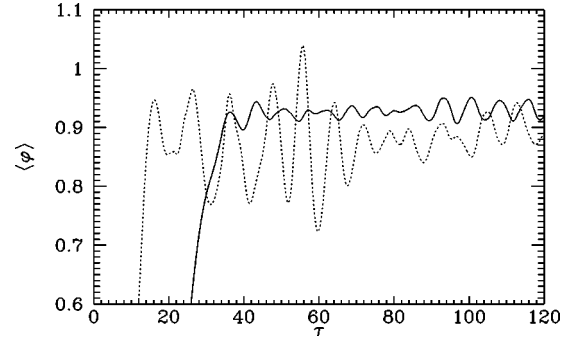


FIG. 3. Time dependence of the zero-momentum mode, $\varphi_0 = \langle \phi \rangle$. The dotted line corresponds to initial bubble separation of $l/2\pi=4$, the solid line corresponds to $l/2\pi=8$.

slightly with τ , which is the sign of ongoing relaxation. We do not present results for $l/2\pi=10$ and $l/2\pi=12$ since they do not differ appreciably from the case $l/2\pi=8$ (φ_0 at $l/2\pi=12$ is larger by an about 0.01 than the corresponding value for $l/2\pi=8$).

The deviation of φ_0 from the vacuum value is not unexpected since a random field of classical waves is created after the bubble collision, i.e., $\text{Var}(\phi) \equiv \langle \phi^2 \rangle - \langle \phi \rangle^2$, is nonzero. The time dependence of the variance is shown in Fig. 4. Note again that with fixed initial conditions the variance does not depend upon λ ; i.e., it has a nonthermal origin.

At $\tau \sim 80$, with $l/2\pi=8$ we have $\text{Var}(\phi) \approx 0.036$ and with $l/2\pi=4$ we find $\text{Var}(\phi) \approx 0.08$. Again we employ time averaging over several oscillations. At small λ those values are much larger than its equivalent LTE value $\text{Var}(\phi) = T_{\text{LTE}}^2/12$ [see Eq. (5)]. The fact that $\text{Var}(\phi)$ in NEQ can exceed its equivalent LTE value by many orders of magnitude was the main point of Ref. [2] which studied the preheating phase after inflation and of Ref. [9] which studied conditions following bubble collisions. Our work supports the claim in Ref. [9] that NEQ phase transitions can occur in models which contain more degrees of freedom than the simple toy model of Eq. (1).

Let us see whether we can understand the deviation of the zero mode from its vacuum value by the existence of a non-zero $\text{Var}(\phi)$. Let us decompose the field as $\phi = \varphi_0 + \delta\phi$, and substitute this decomposition into the equation $dV/d\phi=0$. We find, in the Hartree approximation,

$$(\varphi_m + 3\langle \delta\phi^2 \rangle)\varphi_0 - (1 + \varphi_m)\varphi_0^2 + \varphi_0^3 - (1 + \varphi_m)\langle \delta\phi^2 \rangle = 0. \quad (10)$$

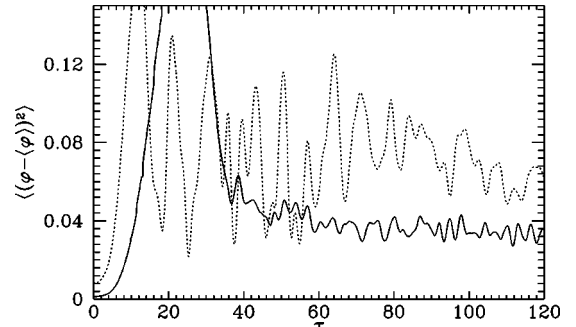


FIG. 4. Time dependence of the variance, $\langle \phi^2 \rangle - \langle \phi \rangle^2$. The dotted line corresponds to initial bubble separation of $l/2\pi=4$ and the solid line corresponds to $l/2\pi=8$.

Assuming in addition the deviation of φ_0 from 1 to be small, we find

$$\varphi_0 = 1 - \frac{2 - \varphi_m}{1 - \varphi_m + 3\langle\delta\varphi^2\rangle}\langle\delta\varphi^2\rangle. \quad (11)$$

Using $\varphi_m = 0.1$ and the values of $\langle\delta\varphi^2\rangle$ inferred from Fig. 4, we find $\varphi_0 = 0.93$ for $l/2\pi = 8$ and $\varphi_0 = 0.87$ for $l/2\pi = 4$, which are in excellent agreement with the results presented in Fig. 3.

We can also understand the dependence upon l , the initial bubble separation. The larger the initial bubble separation, the longer bubbles will expand before they collide. As a bubble expands, its wall thickness decreases. Hence, colliding bubbles in the $l/2\pi = 8$ calculation are thinner than in the $l/2\pi = 4$ case. Following the discussion in Ref. [9], we expect the average energy of the quanta created in wall collisions to scale as Δ^{-1} , where Δ is the wall thickness at collision. Since the effect of the background on the effective potential scales as $n/E \propto \Delta$, we expect the $l/2\pi = 4$ calculation to result in a larger departure from the vacuum value. This expectation is confirmed by the results shown in the figures.

Even though we only examine a particularly simple model, we conjecture that a deviation of φ_0 from its thermal equilibrium value in the aftermath of bubble collisions may have important consequences for some applications of first-order phase transitions, e.g., electroweak baryogenesis. In any scenario where the baryon asymmetry is generated during a first-order electroweak phase transition, the asymmetry is generated in the vicinity of bubble walls, and a strong constraint on the ratio between the vacuum expectation value of the Higgs field inside the bubble and the temperature must be imposed, $\langle\phi(T)\rangle/T > 1$ [11]. This bound is necessary for the just created baryon asymmetry to survive the anomalous baryon-number-violating interactions inside the bubble, and

may be translated into a severe upper bound on the physical mass of the scalar Higgs particle. Combining this bound with the CERN e^+e^- collider LEP constraint already rules out the possibility of electroweak baryogenesis in the standard model of electroweak interactions, and even impacts electroweak baryogenesis in the minimal supersymmetric extension of the standard model [12]. Since the rate of anomalous baryon-number-violating processes scales like $\exp(-\langle\phi\rangle/T)$, it is clear that even a small change in the vacuum expectation value of the Higgs scalar field from its equilibrium value may be crucial for electroweak baryogenesis considerations. Our results suggest that imposing the bound $\langle\phi(T)_{\text{EQ}}\rangle/T > 1$ may not be a sufficient condition for successful electroweak baryogenesis. NEQ effects at the completion of the phase transition may reduce the expectation value of the Higgs field, thus enhancing the anomalous baryon-number-violating rate with respect to its equilibrium value, making the upper bound on the Higgs boson mass more severe. Applications of our considerations to the electroweak transition may result in a fatal blow to many scenarios involving extensions of the standard model where the baryon asymmetry is generated during the electroweak phase transitions.

The model we consider in this paper is quite simple, but it illustrates several points. The most important result is that NEQ conditions following bubble collisions can have a dramatic effect upon the effective potential. Although the model we study is too simple to result in symmetry restoration, the numerical results confirm the assumptions made in Ref. [9] about the efficiency of NEQ conditions. We mentioned a possible direct application of our results to electroweak baryogenesis, but we believe that the phenomenon of NEQ effects will have other implications as well.

The work of E.W.K. and A.R. was supported in part by the Department of Energy and by NASA Grant No. NAG 5-2788. I.T. was supported by Department of Energy Grant No. DE-AC02-76ER01545 at Ohio State.

-
- [1] D. A. Kirzhnits and A. D. Linde, Phys. Lett. **42B**, 471 (1972); L. Dolan and R. Jackiw, Phys. Rev. D **9**, 3320 (1979); S. Weinberg, *ibid.* **9**, 3357 (1979).
 - [2] L. Kofman, A. Linde, and A. A. Starobinsky, Phys. Rev. Lett. **76**, 1011 (1996); I. I. Tkachev, Phys. Lett. B **376**, 35 (1996).
 - [3] L. Kofman, A. Linde, and A. A. Starobinsky, Phys. Rev. Lett. **73**, 3195 (1994).
 - [4] J. H. Traschen and R. H. Brandenberger, Phys. Rev. D **42**, 2491 (1990); Y. Shtanov, J. Traschen, and R. Brandenberger, *ibid.* **51**, 5438 (1995); D. Boyanovsky, H. J. de Vega, R. Holman, D.-S. Lee, and A. Singh, *ibid.* **51**, 4419 (1995); D. Boyanovsky, M. D'Attanasio, H. J. de Vega, R. Holman, and D.-S. Lee, *ibid.* **52**, 6805 (1995).
 - [5] S. Khlebnikov and I. Tkachev, Phys. Rev. Lett. **77**, 219 (1996); Phys. Lett. B **390**, 80 (1997); Phys. Rev. Lett. **79**, 1607 (1997); T. Prokopec and T. G. Roos, Phys. Rev. D **55**, 3768 (1997).
 - [6] E. W. Kolb, A. D. Linde, and A. Riotto, Phys. Rev. Lett. **77**, 4290 (1996).
 - [7] G. W. Anderson, A. Linde, and A. Riotto, Phys. Rev. Lett. **77**, 3716 (1996); G. Dvali and A. Riotto, Phys. Lett. B **388**, 247 (1996).
 - [8] S. Y. Khlebnikov and I. I. Tkachev, Phys. Rev. D **56**, 653 (1997).
 - [9] E. W. Kolb and A. Riotto, Phys. Rev. D **55**, 3313 (1997).
 - [10] A. Riotto and I. I. Tkachev, Phys. Lett. B **385**, 57 (1996).
 - [11] For a recent review, see, for instance, V. A. Rubakov and M. E. Shaposhnikov, Usp. Fiz. Nauk. **166**, 493 (1996).
 - [12] M. Carena, M. Quiros, A. Riotto, I. Vilja, and C. Wagner, Fermilab-PUB-96/271-A, hep-ph 9702409.